Mesoscale calcium responses in murine visual cortex

Primary visual cortex (V1) in mice contains neurons sensitive to position, orientation, …

Higher visual areas (HVAs)

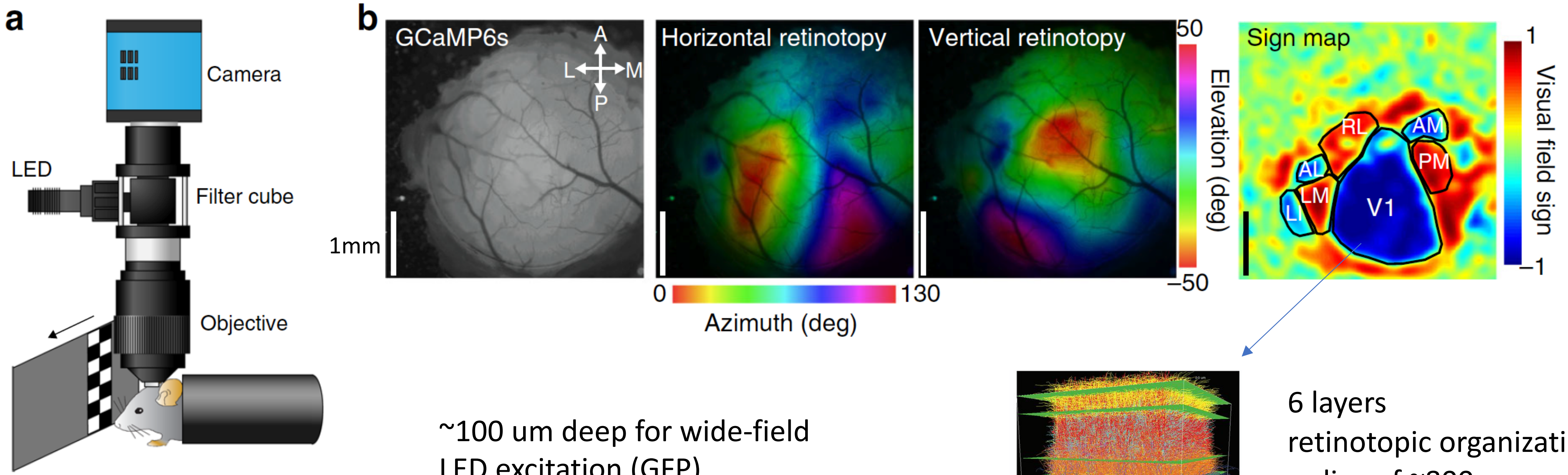

~100 um deep for wide-field
LED excitation (GFP)
4mm X 4mm (400 X 400 px), CMOS

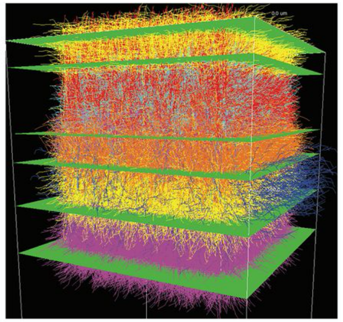

6 layers
retinotopic organization
radius of ~800 um
~230k neurons

Distributed and retinotopically asymmetric processing of coherent motion in mouse visual cortex. **Nature Communications. 2020**

Mesoscale calcium responses in murine visual cortex

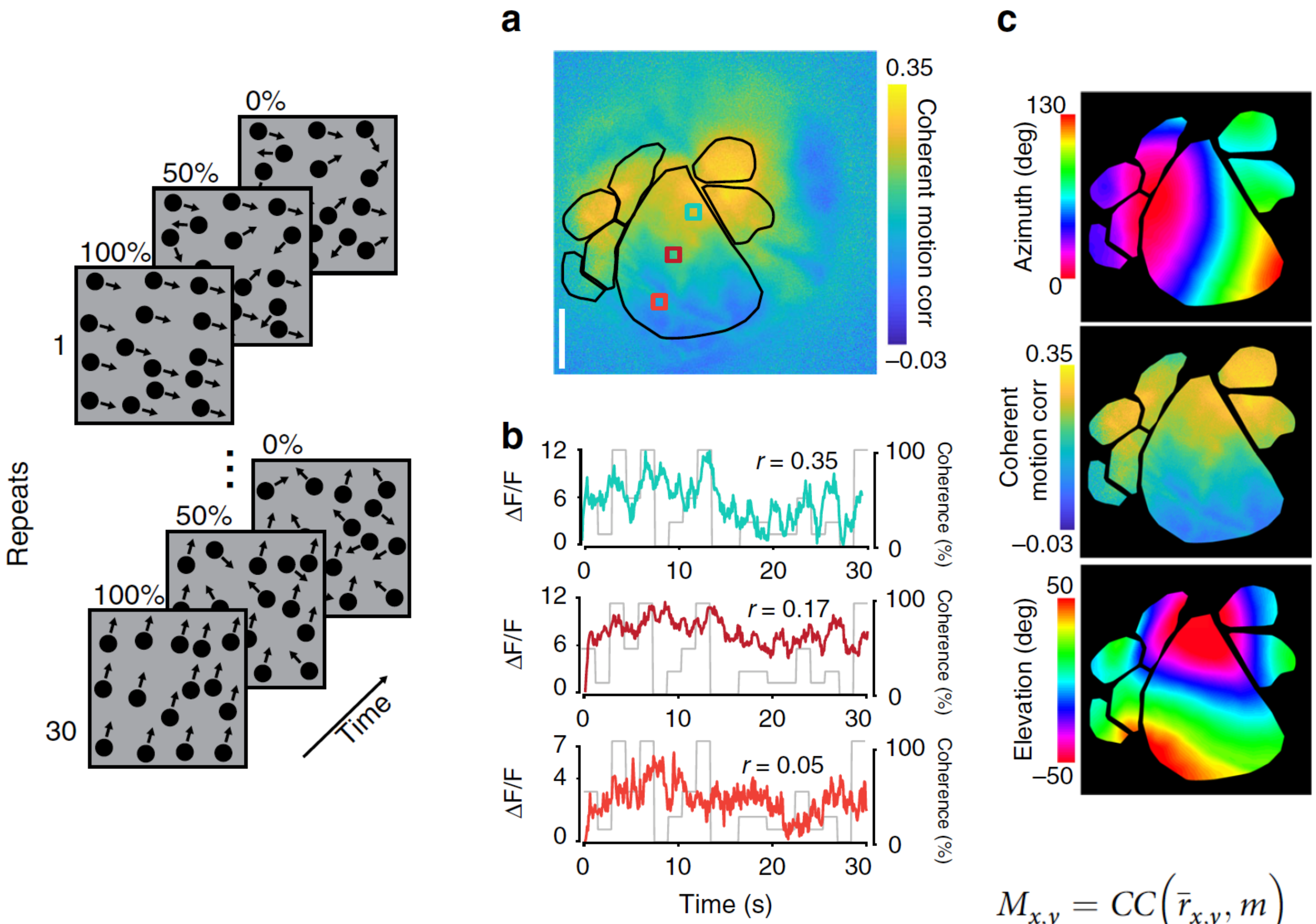

$$M_{x,y} = CC\left(\bar{r}_{x,y}, m\right)$$

Distributed and retinotopically asymmetric processing of coherent motion in mouse visual cortex. **Nature Communications. 2020**

Population decoding in V1

V1 has a retinotopic organization - it is composed of simple and complex cells distinguished by their ***receptive field***

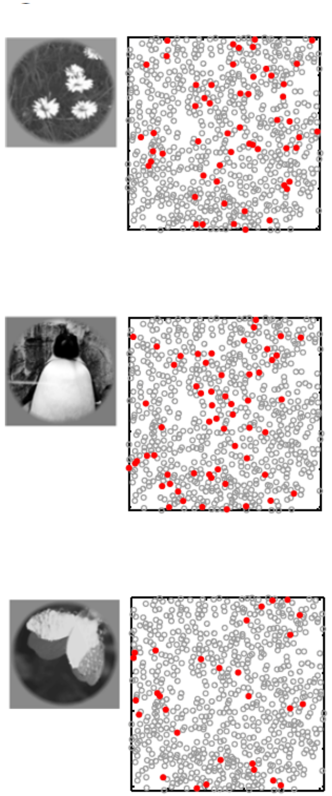

$$D(x,y) = \frac{1}{2\pi\sigma_x\sigma_y}\exp\left(-\frac{x^2}{2\sigma_x^2}-\frac{y^2}{2\sigma_y^2}\right)\cos(kx-\varphi)$$

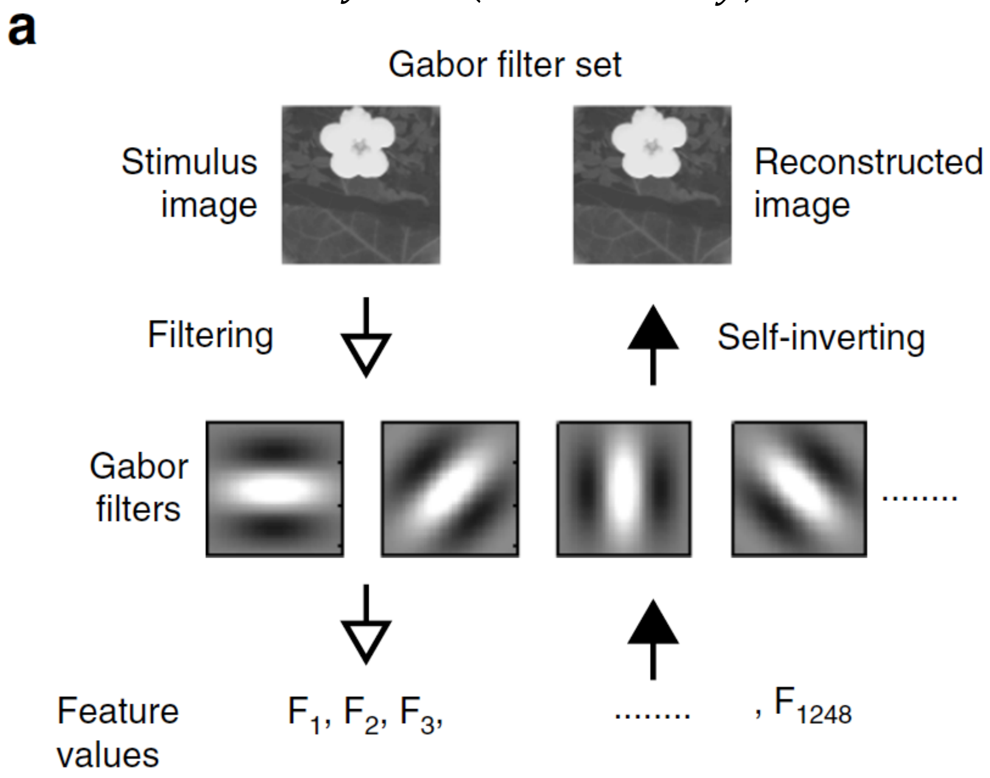

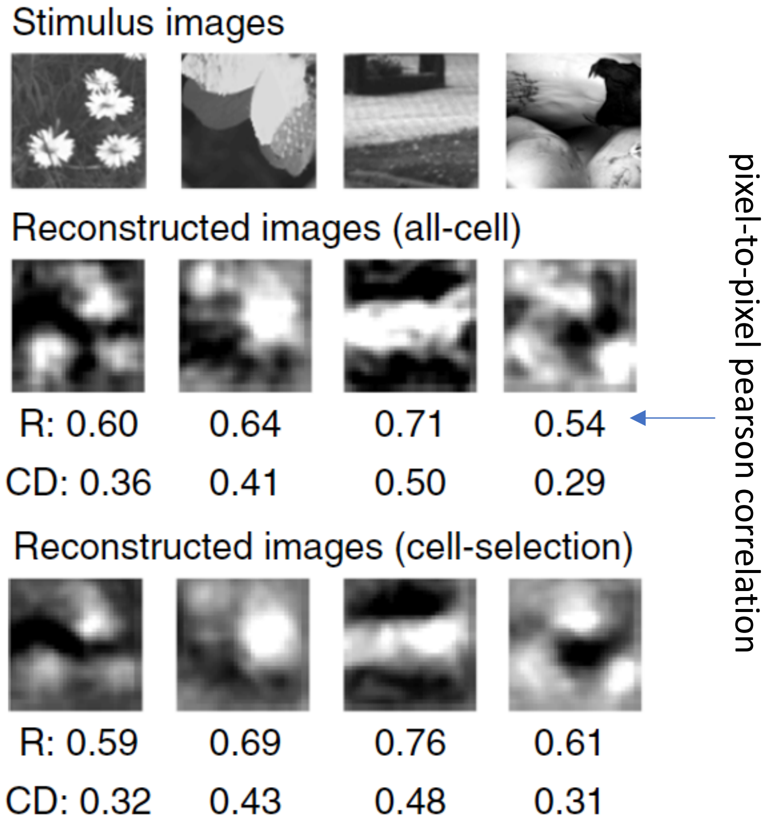

560 (284-712) cells/plane – median (25^{th}-75^{th} percentile)

2D two-photon imaging of GCaMP6s in mouse V1. 920nm excitation, FOV: (338 X 338 um) @ 30Hz

Natural images are reliably represented by sparse and variable populations of neurons in the visual cortex. **Nature Communications. 2020**

Spatial domain

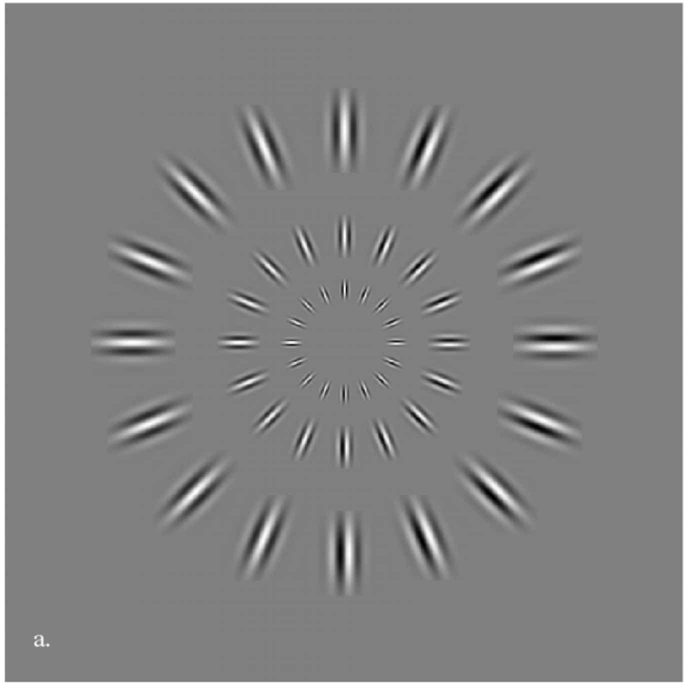

Frequency domain

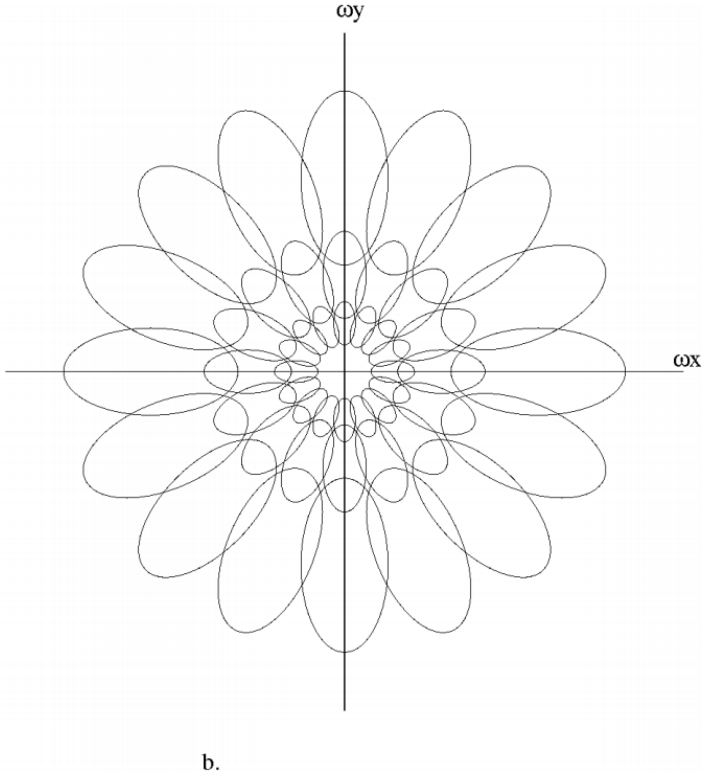

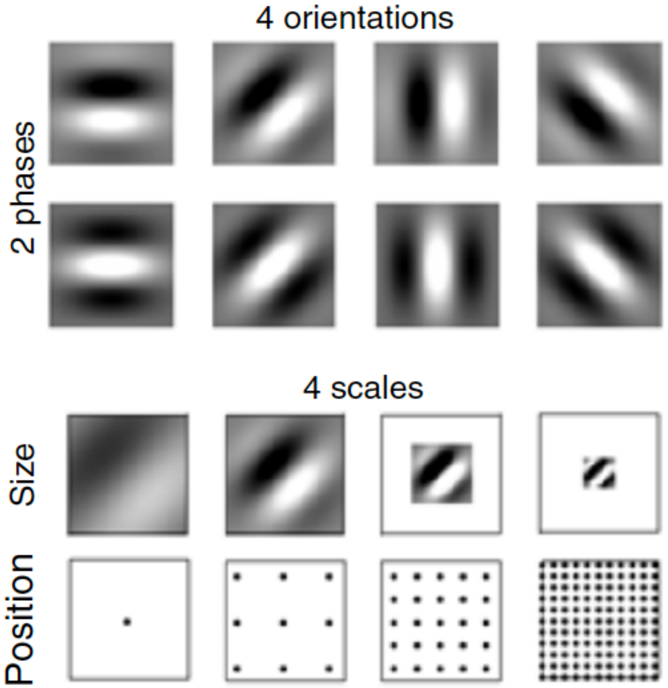

8 + 9***8** + 25***8** + 121***8** = 1248

$\lambda = 1.5 - 2.0$ for simple cells, HMB ~1.5 octaves

Wave vector is orthogonal to major axis

inverse prop to spatial frequency

HMB [octaves]

$$\sigma = \frac{\kappa}{\omega_o} \quad \text{where} \quad \kappa = \sqrt{2\ln 2}\left(\frac{2^{\phi}+1}{2^{\phi}-1}\right)$$

Space is a lattice with spacing $\boldsymbol{a_0^m} b_0$

scale dependent spacing

a_0^m is related to σ, b_0 is the spatial unit

Image representation using 2D Gabor wavelets. **IEEE. 1996**

Image reconstruction experiments

TABLE 1
FRAME BOUNDS FOR THE 2D GABOR WAVELETS WITH 1.5 OCTAVE BANDWIDTH FOR DIFFERENT NUMBERS OF SAMPLING ORIENTATIONS (K), WITH THE NUMBER OF FREQUENCY STEPS PER OCTAVE N = 1 AND N = 3, AND THE UNIT SPATIAL SAMPLING INTERVAL $b_o = \Delta x/a_o = 0.8$

N = 1

K	A	B	B/A
4	2.502	54.388	21.739
6	17.131	56.965	3.325
8	32.107	62.141	1.935
12	57.150	81.810	1.432
16	78.494	107.516	1.370
20	98.499	134.178	1.362

N = 3

K	A	B	B/A
4	19.273	136.424	7.079
6	67.908	144.066	2.122
8	118.664	161.044	1.357
12	201.665	217.529	1.079
16	272.766	286.155	1.049
20	341.454	357.199	1.046

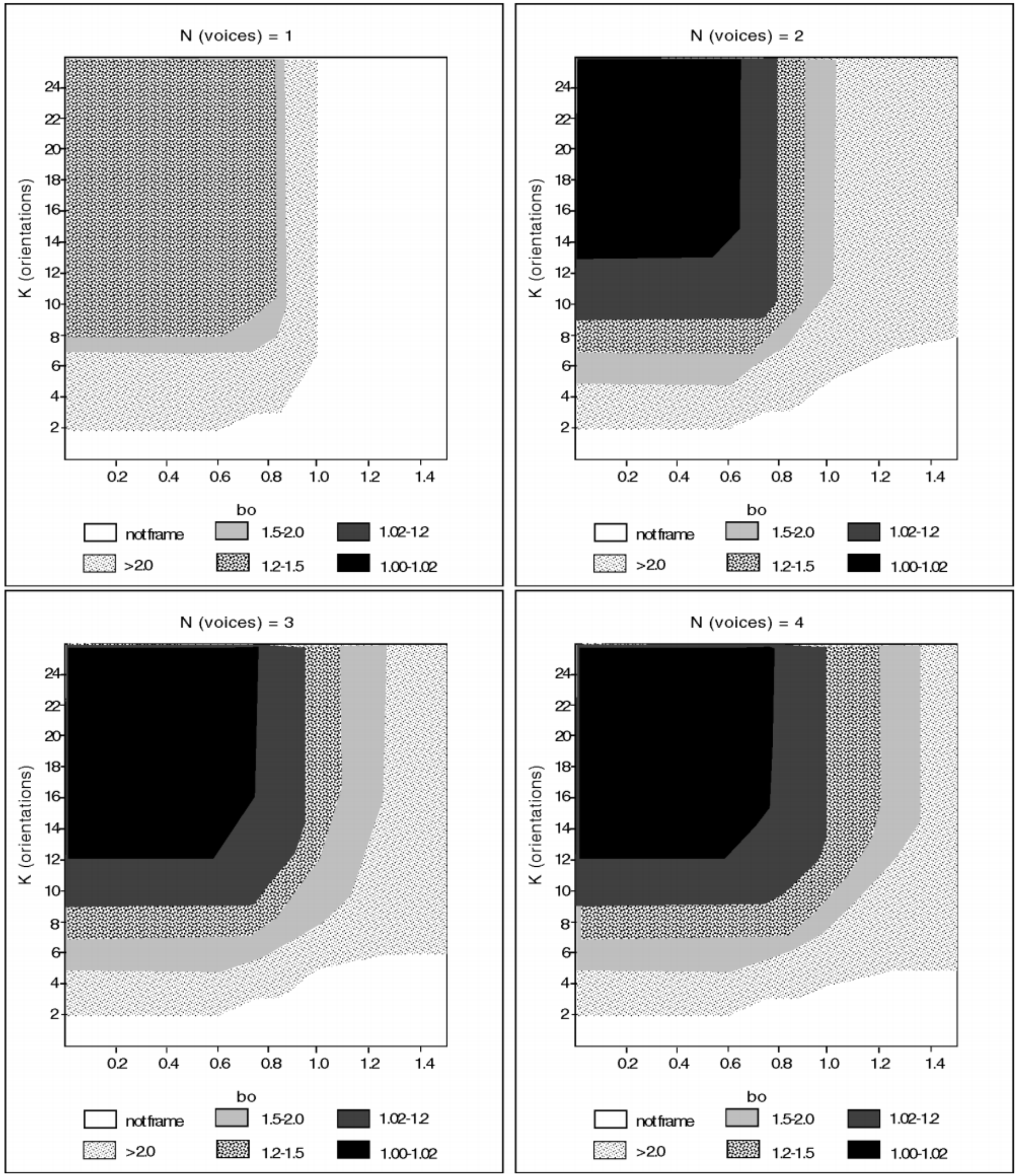

B/A = 1 is a “tight-frame” which achieves perfect reconstruction

Image representation using 2D Gabor wavelets. **IEEE. 1996**

TABLE 1 | Estimates of Cortical Density.

Region	Neuron density	Non-neuronal cell density	Total cell density	Interneuron subtypes	Astrocytes	Oligodendrocytes	Microglia
Cortex (General)	92,000 (Schüz and Palm, 1989)	43,000 (Tsai et al., 2009)	127,870 (Murakami et al., 2018)	2,903 PV, 4,877 SST, 1,935 VIP (Kim et al., 2017)	15,696 S-100β (Grosche et al., 2013)	12,500 (Rockland and DeFelipe, 2012)	6,500 (Nimmerjahn et al., 2005) 6,500 (Lawson et al., 1990)
Frontal cortex	66,771* 104,000 (Rajkowska et al., 2016) 123,000 (Schmid et al., 2013) 190,000 (Rockel et al., 1980) **Mean and STD:** **121,000 ± 52,000**	79,393*	104,100 (Murakami et al., 2018)	863 PV, 1,749 SST, 2,598 VIP (Kim et al., 2017)	7,000 GFAP+ (Xu et al., 2007) 52,000 GFAP+ (Rajkowska et al., 2016) **Mean and STD:** **29,500 ± 31,820**	87,803 (Duque et al., 2012)	6,200 (Lawson et al., 1990)
Posterior parietal association areas	76,588* 230,000 (Rockel et al., 1980) **Mean and STD:** **150,000 ± 100,000**	115,318*	150,530 (Murakami et al., 2018)	4,452 PV, 5,140 SST, 2,512 VIP (Kim et al., 2017)	–	—	6,124 (San Jose et al., 2001) 6,900 (Lawson et al., 1990) **Mean and STD:** **6,512 ± 549**
Visual areas	155,426* 214,000 (Rockel et al., 1980) 92,400 (Cragg, 1967) 194,000 (Heumann et al., 1977) **Mean and STD:** **164,000 ± 50000**	169,804*	145,170 (Murakami et al., 2018)	4,886 PV, 5,028 SST, 2,964 VIP (Kim et al., 2017)	49,600 S-100β (Argandoña et al., 2009)	10,000 (Tremblay et al., 2012)	7,250 (Tremblay et al., 2012)

cells/mm^3

Effect of stimulus image size/orientation

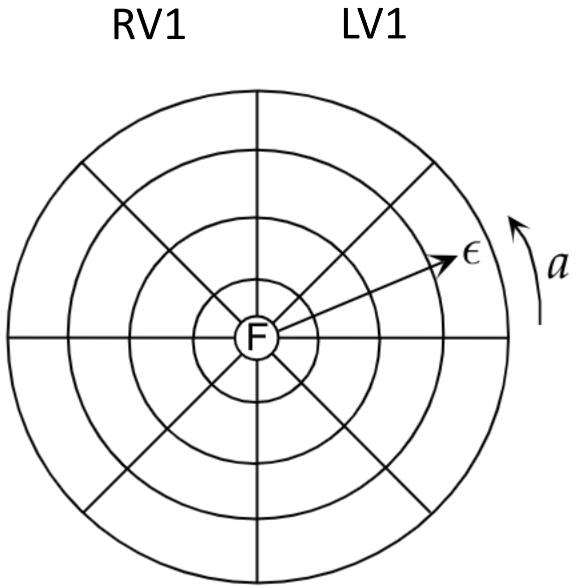

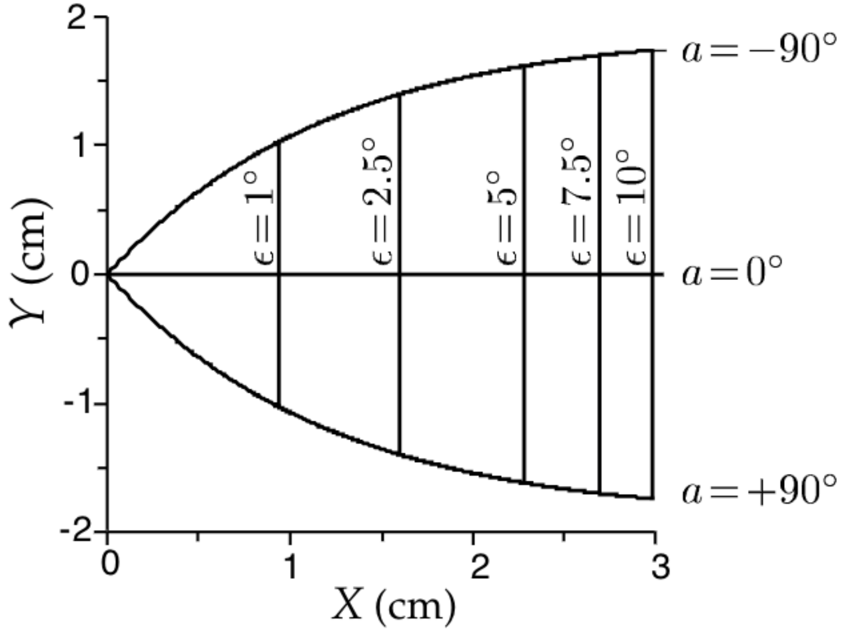

$$\frac{\varepsilon}{d}\frac{180}{\pi} \qquad \frac{a}{d}\frac{180}{\pi}$$

Let (X, Y) be cortex coordinates

$$X = \boldsymbol{\lambda} \ln(1 + \epsilon/\epsilon_0)$$

$$Y = -\frac{\boldsymbol{\lambda}\epsilon a \pi}{(\epsilon + \epsilon_0)180}$$

$\boldsymbol{\lambda}$ = 12mm (macaque)

ε_0 = 1^o

Scaling or rotation is translation on the cortical surface

Theoretical Neuroscience. Wiley

Breaking down an existing system

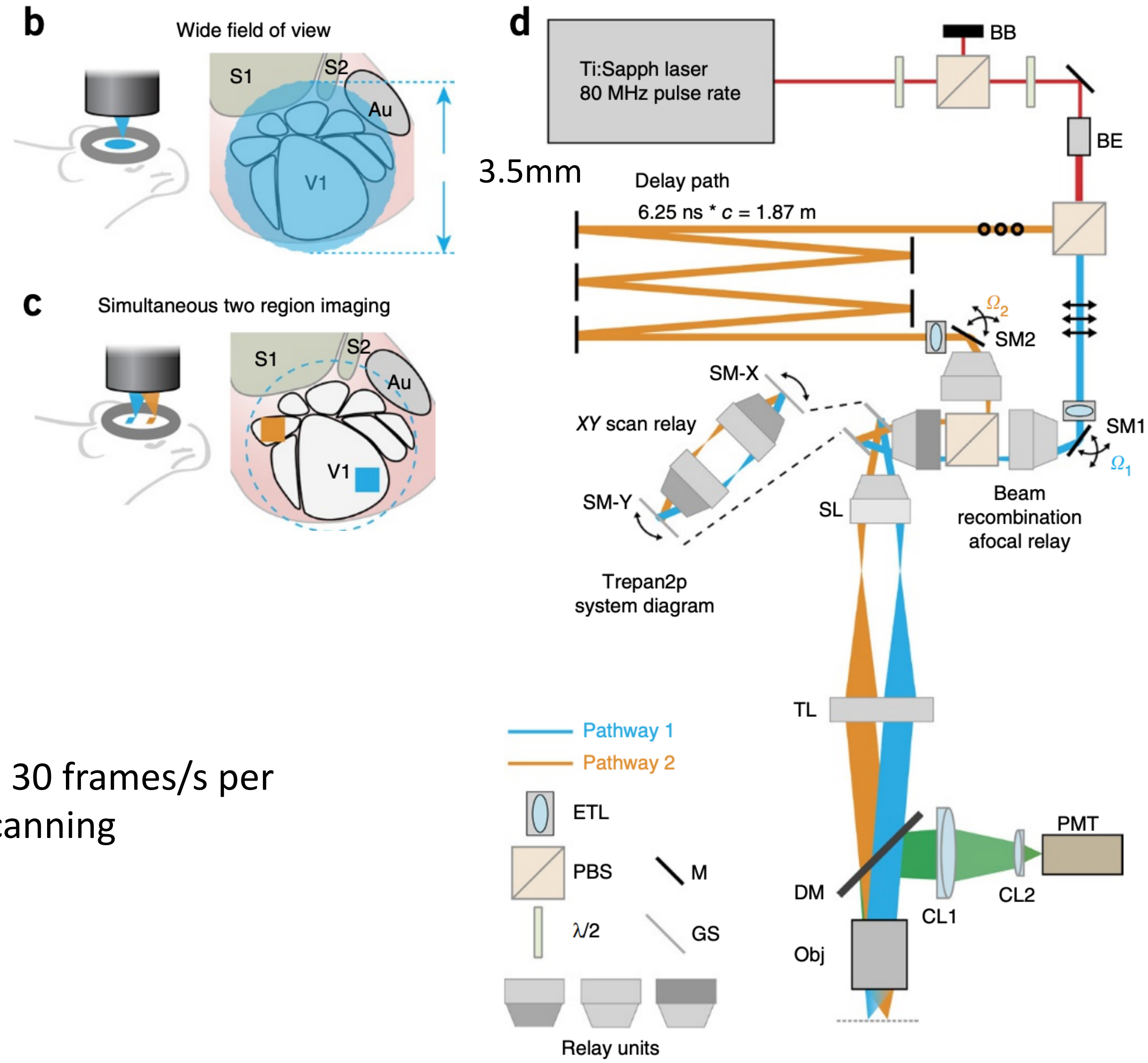

512 x 256 pixels @ 30 frames/s per region, 2D galvo scanning

Wide field-of-view, multi-region, two photon imaging of neuronal activity in the mammalian brain. **Nature Biotechnology. 2016**

Efficient Coding Hypothesis: Sensory systems have evolved to transmit maximal information about incoming signals given internal resource constraints (noise, metabolic cost)

Information Bottleneck (IB): Encode *X* to maximize fidelity while constraining the **coding capacity**

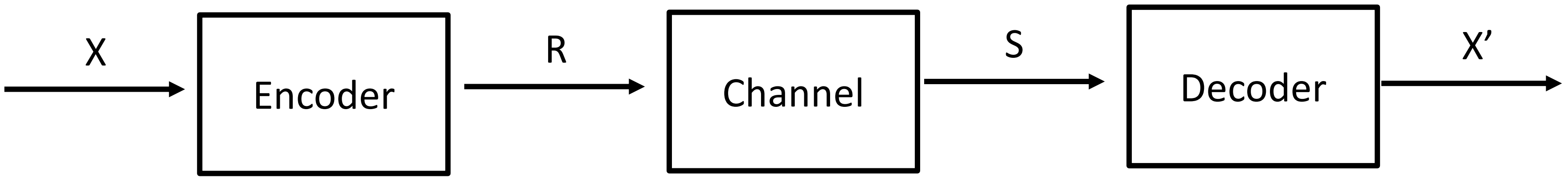

Goal of the paper: Unify efficient coding hypothesis with predictive and sparse coding

Toward a unified theory of efficient, predictive, and sparse coding. **PNAS. 2018**

Using IB to predict neural responses

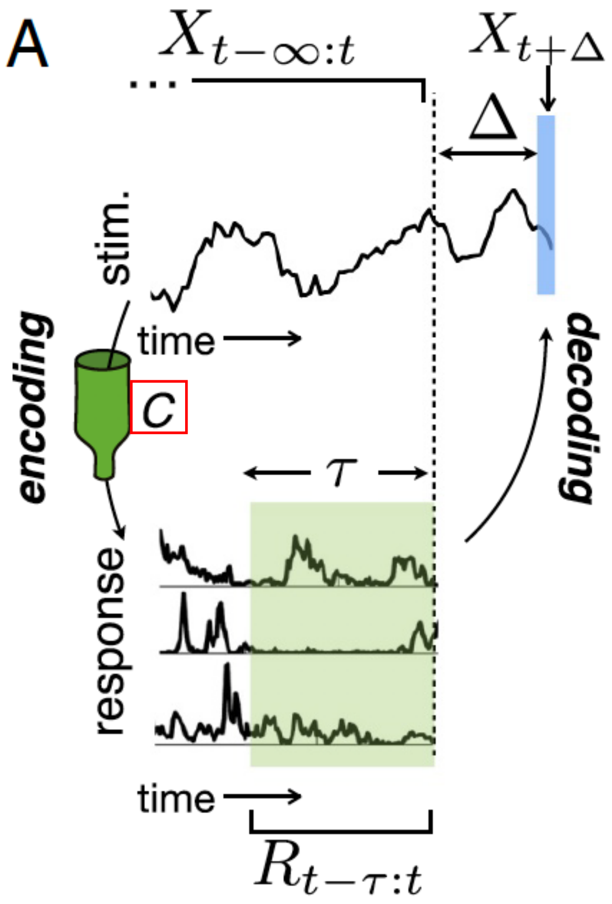

Parameter space

Encoding filters

$\tau = 0$

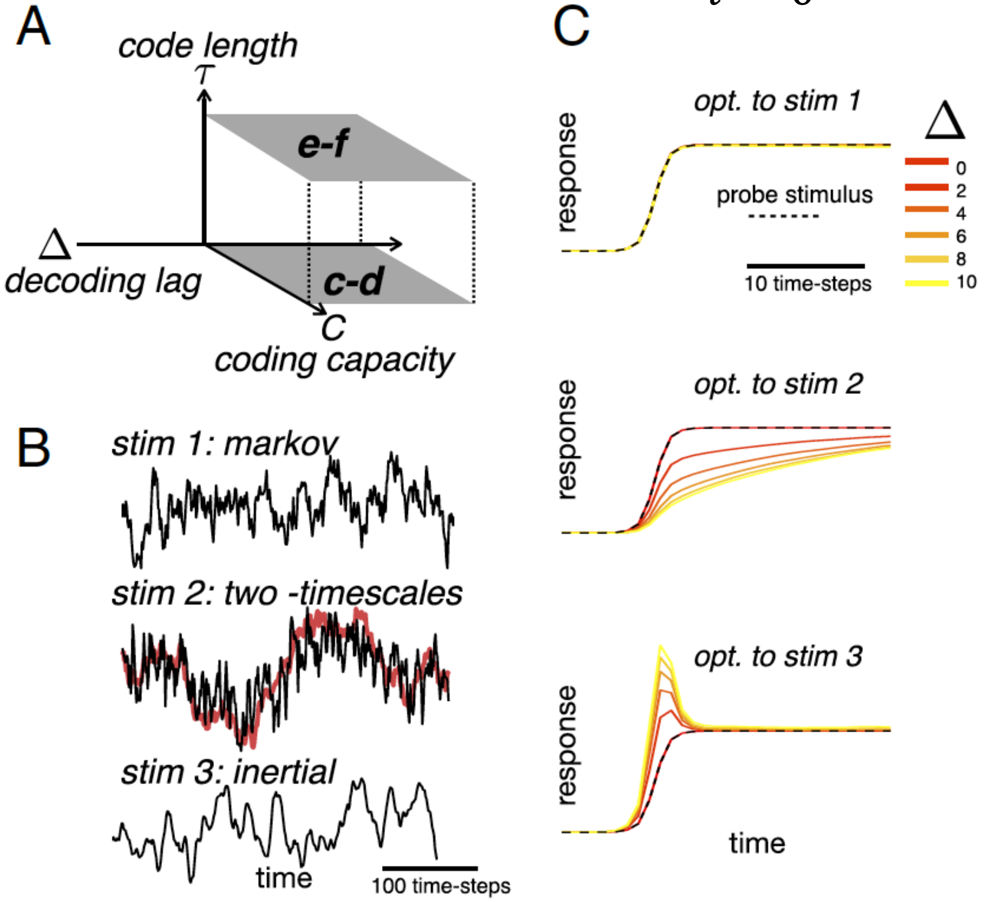

Low-pass

High-pass

τ – code length, ≥ 0

Δ – lag time

C – coding capacity (relates to SNR, determines number of neurons)

Toward a unified theory of efficient, predictive, and sparse coding. **PNAS. 2018**